

## Hg<sup>2+</sup> wettability and fluorescence dual-signal responsive switch based on a cysteine complex of piperidine-calix[4]arene†

Xiaoyan Zhang, Haiyang Zhao, Xianliang Cao, Ningmei Feng, Demei Tian and Haibing Li\*

Cite this: *Org. Biomol. Chem.*, 2013, **11**, 8262

Received 3rd September 2013,  
Accepted 3rd October 2013

DOI: 10.1039/c3ob41794h

[www.rsc.org/obc](http://www.rsc.org/obc)

The recognition of the mercury(II) ion (Hg<sup>2+</sup>) is essential because of its extreme toxicity in the environment and food. Hence we reported a novel cysteine (Cys) complex of piperidine-calix[4]arene (L) as a convenient and effective dual-signal responsive switch for Hg<sup>2+</sup>. This switch system exhibited excellent selectivity toward Hg<sup>2+</sup> by fluorescence (FL), <sup>1</sup>H NMR spectroscopy and the atomic force microscopy (AFM). More importantly, the Hg<sup>2+</sup>-responsive switch had an important and potential application by water contact angle (CA) on a functional micro-nano silicon surface, including intelligent microfluidic and laboratory-on-chip devices, controllable drug delivery, and self-cleaning surfaces.

### Introduction

Mercury (Hg) is a non-essential element of living, which is associated with chemical substances: metallic mercury, inorganic and organic mercury. Among them, inorganic mercury such as mercuric sulfide, mercuric chloride and mercuric nitrate can easily pass through the skin, respiratory, and gastrointestinal tissues, which leads to DNA damage, mitosis impairment, and permanent damage to the central nervous system.<sup>1</sup> So the mercury(II) ion (Hg<sup>2+</sup>) is one of the most dangerous and ubiquitous pollutants, which raises serious environmental and health concerns.<sup>2</sup> At present, the “on-off” fluorescent probe is an extraordinarily common method to recognize Hg<sup>2+</sup>. For example, Mandal *et al.* described a novel imine-based receptor as a turn-on fluorescence response for the detection of Hg<sup>2+</sup> in aqueous media.<sup>3</sup> Wu *et al.* have reported a novel “off-on” fluorescent probe based on rhodamine for the detection of Hg<sup>2+</sup> in aqueous solution.<sup>4</sup> However, all of the above fluorescent switches were just a single output signal in the solution phase. Accordingly, the development of a Hg<sup>2+</sup> dual-signal responsive switch has attracted great interest because of potential applications as chips or materials which could detect environmental pollution.

Wettable responsive switches on the functional surface that can be reversibly changed between a hydrophobic character

and a hydrophilic character have aroused great attention due to a wide range of potential applications, including intelligent microfluidic and laboratory-on-chip devices, controllable drug delivery, and self-cleaning surfaces.<sup>5</sup> Many external stimuli, such as pH, light, temperature, electric potential and solvents, exhibit excellent and reversible wettability on the functional surfaces.<sup>6</sup> Among them, the design and synthesis of response molecules play a key role in constructing wettable functional surfaces. As is known to all, the calixarene with a “cup-like” shape as the third generation of supramolecules has an important application, because its cavity is adjustable by varying the shape and size or by modifying the substituents of the upper and lower rims.<sup>7</sup> They are widely applied as complexing reagents for many metals, organic molecules, and drugs.<sup>8</sup> Just recently, we reported a switchable wettability sensor for ion pairs based on calix[4]azacrown by the click reaction on a silicon surface.<sup>9</sup> Compared with responsive wettability surfaces for recognizing small molecules, surfaces for recognizing cations have been barely reported. This may be because the cations themselves are without hydrophilic or hydrophobic groups. Considering that, we can detect cations through the synergy between functional surfaces based on calixarenes and some substances with hydrophilic and hydrophobic groups. Cys is a heavy metal detoxification agent due to its strong binding affinity toward Hg<sup>2+</sup>.<sup>10</sup> The affinity is closely related with the interaction of Hg<sup>2+</sup> and sulfhydryl (–SH) groups. Therefore, we designed a wettable responsive switch based on a calixarene receptor and Cys complex for the recognition of Hg<sup>2+</sup>. As a consequence of its outstanding properties, the Hg<sup>2+</sup>-responsive switch based on the calixarene and Cys complex has formed attractive applications in many fields,

Key Laboratory of Pesticide and Chemical Biology (CCNU), Ministry of Education, College of Chemistry, Central China Normal University, Wuhan, 430079, P. R. China. E-mail: [lhbing@mail.ccnu.edu.cn](mailto:lhbing@mail.ccnu.edu.cn); Fax: (+86) 27 67866423

† Electronic supplementary information (ESI) available: Characterized (EIS, IR, CA); copies of NMR of new compounds. See DOI: 10.1039/c3ob41794h

especially on a silicon surface. To the best of our knowledge, a  $\text{Hg}^{2+}$  wettability and fluorescence dual-signal responsive switch has been largely unexplored.

In order to achieve this goal, we synthesized a novel deep cavity of calix[4]arene with piperidine groups as the upper rim (**L**). On the basis of the interaction between the piperidine groups and Cys, we obtained an  $[\text{L} + \text{Cys}]$  complex with a conjugation ratio of 1 : 1, by FL,  $^1\text{H}$  NMR spectroscopy and density functional calculations (DFT) studies. Further, the *in situ*  $[\text{L} + \text{Cys}]$  complex was added to 7 important heavy metal ions, *viz.*,  $\text{Hg}^{2+}$ ,  $\text{Pb}^{2+}$ ,  $\text{Cd}^{2+}$ ,  $\text{Cu}^{2+}$ ,  $\text{Ni}^{2+}$ ,  $\text{Zn}^{2+}$  and  $\text{Ba}^{2+}$ . From this it was then found that this complex acted as a recognition ensemble toward  $\text{Hg}^{2+}$ , by switch-off fluorescence,  $^1\text{H}$  NMR spectroscopy and AFM. Even further, the  $\text{Hg}^{2+}$ -responsive switch based on the  $[\text{L} + \text{Cys}]$  complex had been successfully applied on a functional micro-nano silicon surface by the simple click reaction.<sup>11</sup> Moreover, the  $[\text{L} + \text{Cys}]$  complex could act as a convenient and effective wettability switch for  $\text{Hg}^{2+}$  by its contact angle (CA) measurement on the silicon surface.

## Results and discussion

The synthetic strategy for the complex **L** was depicted in Scheme 1. Calix[4]arene (C4DT) and sodium methylate were stirred and refluxed in acetonitrile for 0.5 h, and then propargyl bromide was added.<sup>12</sup> The mixture was stirred at room temperature for 8 h, and the crude product was purified by column chromatography to afford propargyl-calix[4]arene (C4AM) (Fig. S1†) in 85% yield. Subsequently, C4AM, piperidine, formaldehyde and acetic acid were stirred in THF at room temperature for 48 h.<sup>13</sup> The evaporated crude product was then purified by column chromatography to give a white powder (**L**) in 86% yield. Complex **L** was totally characterized by NMR (Fig. S2 and S3†) and ESI-MS (Fig. S4†). As shown in Fig. S2†, the  $^1\text{H}$  NMR spectrum of **L** exhibited a pair of doublets for the bridging methylene groups at 4.06 and 4.48 ppm, a single peak for the alkynyl group at 2.61 ppm, and then two singlets for the piperidine groups at 1.40 and 1.53 ppm. All of these indicated the cone conformation of **L**. The  $^{13}\text{C}$  NMR spectrum data further corroborated the cone conformation of **L** in the presence of a peak for the methylene resonances. At the same time, the *m/z* peak of **L** was at 753 in the ESI mass spectrum.

To provide support for the binding between **L** and Cys, and then the removal of Cys from the  $[\text{L} + \text{Cys}]$  complex by  $\text{Hg}^{2+}$ , some verifying experiments were done in the solution phase. First of all, a fluorescence experiment of the selective

recognition for  $\text{Hg}^{2+}$  was carried out using an excitation wavelength of 350 nm. The Cys receptor property of **L** was explored by fluorescence experiments and absorption titrations of the  $[\text{L} + \text{Cys}]$  complex in  $\text{CH}_3\text{CN}-\text{H}_2\text{O}$  solution with 7 different metal ions, including heavy metal ions, *viz.*,  $\text{Hg}^{2+}$ ,  $\text{Pb}^{2+}$ ,  $\text{Cd}^{2+}$ ,  $\text{Cu}^{2+}$ ,  $\text{Ni}^{2+}$ ,  $\text{Zn}^{2+}$  and  $\text{Ba}^{2+}$  with nitrates as counter anion. Since both the receptor **L** and Cys had no fluorescence, the reaction of dansyl chloride and Cys produced sulfa-drug derivatives (Cys-F) which had strong and stable fluorescence signals, as reported in the literature.<sup>14</sup> The fluorescence of Cys-F weakened with the addition of the receptor **L** in  $\text{CH}_3\text{CN}-\text{H}_2\text{O}$  (v/v, 1/1) because of their interaction. This indicated that the  $[\text{L} + \text{Cys}]$  complex was successfully obtained. Subsequently, the selective recognition of 7 different heavy metal ions was monitored by FL. Among all of these ions, only  $\text{Hg}^{2+}$  showed a fluorescence enhancement with the addition of increasing concentrations of this ion, and the enhancement approached (56.6 ± 0.5)-fold at saturation compared with the other metal ions when the titration was carried out in  $\text{CH}_3\text{CN}-\text{H}_2\text{O}$  (v/v, 1/1) (Fig. 1a and 1b). A plot of the relative fluorescence intensity ( $I/I_0$ ) versus the molar ratio ( $n[\text{Hg}^{2+}]/n[\text{L}-\text{Cys}-\text{F}]$ ) suggested a stoichiometric ratio of 1 : 1 between the  $[\text{L} + \text{Cys}]$  complex and  $\text{Hg}^{2+}$ . Furthermore, the binding stoichiometry of the complex formed between **L** and Cys was also 1 : 1 from Job's plot by ultraviolet-visible (UV) spectrum, which had a peak at 286.5 nm with a molar fraction of 0.5 (Fig. S7†). However, when this was titrated with the other metal ions, no fluorescence change was observed (Fig. 1c and Fig. S6†). These results clearly suggested that the  $[\text{L} + \text{Cys}]$  complex could selectively recognize  $\text{Hg}^{2+}$ . The sensitivity of the  $[\text{L} + \text{Cys}]$  complex for  $\text{Hg}^{2+}$  had been evaluated by measuring the lowest detectable concentration. The fluorescence titration was carried out between the  $[\text{L} + \text{Cys}]$  and  $\text{Hg}^{2+}$  by maintaining a 1 : 1 ratio. This showed that 2.00 μM of  $\text{Hg}^{2+}$  is the lowest detectable concentration in  $\text{CH}_3\text{CN}-\text{H}_2\text{O}$  (Fig. S5†).

To further study the interaction of **L** with Cys carried out by  $\text{Hg}^{2+}$ , a fluorescence cycling experiment was done using an excitation wavelength of 350 nm (Fig. 2a). Under the above

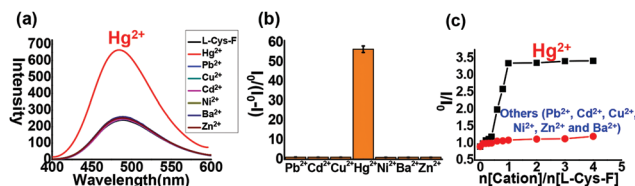
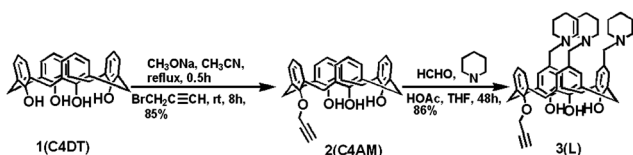


**Fig. 1** (a) FL spectra for the  $[\text{L} + \text{Cys}]$  complex with 7 different metal ions, which showed the highly selective recognition for  $\text{Hg}^{2+}$  based on the  $[\text{L} + \text{Cys}]$  complex in  $\text{CH}_3\text{CN}-\text{H}_2\text{O}$  (v/v, 1/1). Note: all metal salts were nitrates. (b) FL variation  $[\Delta I = (I - I_0) / (I_0 - I)]$  (where  $I_0$  is the FL intensity of **L-Cys-F**) histogram for the  $[\text{L} + \text{Cys}]$  complex with 7 different metal ions at 350 nm. More clearly, this also showed the highly selective recognition for  $\text{Hg}^{2+}$  based on the  $[\text{L} + \text{Cys}]$  complex. (c) Relative fluorescence titration intensity ( $I/I_0$ ) versus molar ratio ( $n[\text{cation}]/n[\text{L}-\text{Cys}-\text{F}]$ ),  $\lambda_{\text{ex}} = 350$  nm. It suggested a stoichiometric ratio of 1 : 1 between the  $[\text{L} + \text{Cys}]$  complex and  $\text{Hg}^{2+}$ , and no fluorescence change was noted when this was titrated with the other metal ions. Note: others stood for  $\text{Pb}^{2+}$ ,  $\text{Cd}^{2+}$ ,  $\text{Cu}^{2+}$ ,  $\text{Ni}^{2+}$ ,  $\text{Zn}^{2+}$  and  $\text{Ba}^{2+}$ .



**Scheme 1** Synthesis of **L**.

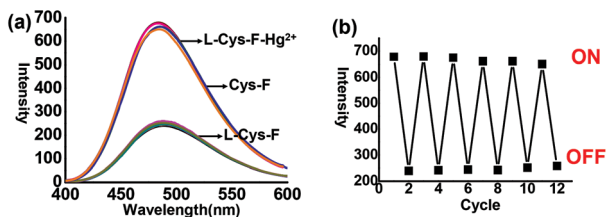


**Fig. 2** (a) The corresponding cycling experiment of the fluorescence. (b) The linear graph of the fluorescence cycle. They showed the fluorescence recovery for 6 switching cycles. Moreover, Cys was carried out by  $\text{Hg}^{2+}$  from the  $[\text{L} + \text{Cys}]$  complex in the solution phase.

conditions, the same equiv. of  $\text{Hg}^{2+}$  was added for its interaction with Cys-F, which showed the fluorescence recovery over 6 switching cycles (Fig. 2b). As there were more errors since the volume of the mixture was gradually increasing, a better fluorescence recovery could not be achieved later.

To obtain further insight into the interaction,  $^1\text{H}$  NMR experiments were completed. The binding of Cys and **L** was studied by  $^1\text{H}$  NMR by keeping a fixed concentration of **L** and Cys to reach up to 2 equiv., respectively. During the study, significant changes which mainly included the chemical shifts of the hydrogen atoms from the piperidine groups were observed in the  $^1\text{H}$  NMR spectra of **L** upon addition of Cys. The result also indicated that the  $[\text{L} + \text{Cys}]$  complex was successfully formed.  $^1\text{H}$  NMR was carried out to support the removal of Cys from the  $[\text{L} + \text{Cys}]$  complex to generate the free **L**. For this purpose, cysteamine (CS) was used instead of Cys because of the poor solubility of the latter when taken in  $\text{DMSO-d}_6$ .<sup>15</sup> During the experiment, the signals corresponding to the complex started to disappear whereas those corresponding to the free **L** started to appear as the concentration of CS was increased (Fig. 3), and thus it clearly supported the removal of Cys from the complex. Further, a 2D NOESY

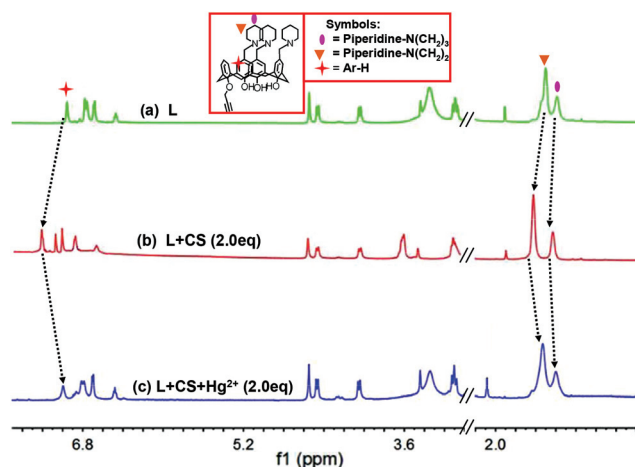


**Fig. 3**  $^1\text{H}$  NMR spectroscopy of (a) **L**, (b)  $[\text{L} + \text{CS}]$  complex, (c)  $[\text{L} + \text{CS}]$  complex with  $\text{Hg}^{2+}$  (cycling experiment of  $^1\text{H}$  NMR spectroscopy), which showed the interaction **L** with Cys carried out by  $\text{Hg}^{2+}$  (DMSO, 600 MHz, 298 K). Note: cysteamine (CS) was used instead of Cys because of the poor solubility of the latter when taken in  $\text{DMSO-d}_6$ .

spectrum (Fig. S9<sup>†</sup>) revealed intermolecular nuclear Overhauser effects (NOEs) between the piperidine groups of **L** and the  $-\text{CH}_2$  groups of CS, which showed that the  $-\text{NH}_2$  moiety of CS had an interaction with the piperidine groups of **L** instead of the sulfhydryl ( $-\text{SH}$ ) moiety of CS.

To understand how the microscopic structural features of **L** differed from its *in situ* complex and the complex with  $\text{Hg}^{2+}$ , atomic force microscopy (AFM) techniques were used. AFM images of **L**, the  $[\text{L} + \text{Cys}]$  complex and the complex with  $\text{Hg}^{2+}$  demonstrated that the particles were well distributed over the mica sheet. The morphological features of **L** alone and in the presence of Cys were quite different in terms of size. Complex **L** alone formed spherical particles of 270–370 nm in size. However, the  $[\text{L} + \text{Cys}]$  complex was 130–230 nm in size. Furthermore, the  $[\text{L} + \text{Cys}]$  complex with  $\text{Hg}^{2+}$  produced uniform spherical particles of 230–330 nm. The spherical particle sizes of the  $[\text{L} + \text{Cys}]$  complex with  $\text{Hg}^{2+}$  were similar to those of **L** only, which also showed that Cys was removed from the  $[\text{L} + \text{Cys}]$  complex by  $\text{Hg}^{2+}$  (Fig. 4).

Further, the binding of **L** and Cys was also examined by computational calculations at the B3LYP/6-31G(d) level using Gaussian03.<sup>16</sup> Partial hydrogen atoms of the host and guest were omitted for clarity. The host **L** was yellow, the guest Cys was purple, oxygen atoms were red, nitrogen atoms were blue, sulfur atoms were dark yellow, and hydrogen atoms were white. The results from the molecular mechanics calculations were generally consistent with FL,  $^1\text{H}$  NMR and AFM experimental results. Fig. 5 shows the top and side views of the optimized structure of the host-guest complex. According to the calculation formula  $\Delta E(\text{binding energy}) = E(\text{host} + \text{guest}) - [E(\text{host}) + E(\text{guest})]$ , the binding energy values for the two processes in which the  $-\text{SH}$  groups of Cys were placed in the bottom and upper of **L** were  $-0.0183468$  a.u. and  $-40.3052274$  a.u. (Fig. S10<sup>†</sup>), respectively. Comparing above binding energies, the stable structure was that of the carboxyl inserted into the lower rim of the cavity and the sulfhydryl exposed outside the cavity of **L** (Fig. 5).

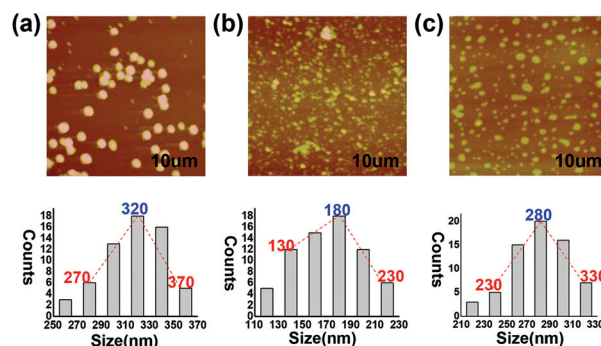


**Fig. 4** AFM images and corresponding particle size distribution plots of (a) **L**, (b)  $[\text{L} + \text{Cys}]$  complex, and (c)  $[\text{L} + \text{Cys}] + \text{Hg}^{2+}$ . Complex **L** alone formed spherical particles of 270–370 nm in size; however, the  $[\text{L} + \text{Cys}]$  complex particles were 130–230 nm in size. Furthermore, the  $[\text{L} + \text{Cys}]$  complex with  $\text{Hg}^{2+}$  produced uniform spherical particles of 230–330 nm. This size range was just similar to **L** alone, which also showed that Cys was removed by  $\text{Hg}^{2+}$  from the  $[\text{L} + \text{Cys}]$  complex.

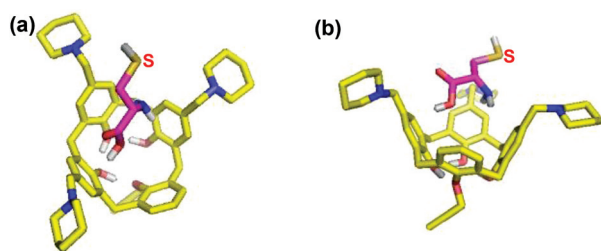


**Fig. 5** (a) The top view on the optimized structure of the [L + Cys] complex. (b) The side view on the optimized structure of the [L + Cys] complex. The stable structure was that the carboxyl inserted into the lower rim of the cavity and the sulfhydryl exposed outside the cavity of L.

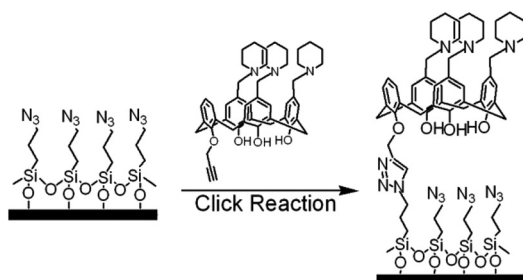


**Fig. 6** The formation process of the functional L-SAM, which indicated that L was successfully modified on a silicon surface by the click reaction.

More importantly, the  $\text{Hg}^{2+}$ -responsive switch had an important and potential application by measurement of the contact angle (CA) on a functional micro-nano silicon surface. Because micro/nano structured and functional silicon surfaces can amplify the signal output with respect to the alteration of wettability,<sup>17</sup> it could reversibly switch Cys and  $\text{Hg}^{2+}$  between a hydrophobic character and a hydrophilic character. At first, the L-SAMs (self-assembled monolayers) were constructed by the click reaction between the Si-N<sub>3</sub> SAMs and L in ethanol (Fig. 6 and Fig. S11†).

The properties of the L-immobilized silicon surfaces were studied by CA. The bare rough silicon wafer was superhydrophilic ( $5.0 \pm 2.0^\circ$ ) (Fig. S12†) and the CA for the Si-N<sub>3</sub>-immobilized surface was  $74.6 \pm 2.0^\circ$ . After the click reaction, the L-SAMs surface became hydrophobic ( $122.6 \pm 2.0^\circ$ ) (Fig. 7a) because of the hydrophobic properties of the piperidine moieties within L. Therefore, we concluded that the functional L-SAMs were constructed perfectly.

The L-modified silicon surfaces were characterized by X-ray photoelectron spectroscopy (XPS) and CA measurements (Fig. S13†). The concentration of carbon had a significant increase and the concentration of oxygen had an obvious decrease in the XPS-derived atomic concentration analysis for the SAMs after the click reaction. This indicated that the click reaction had occurred.

Through scanning electron microscopy (SEM), the rough substrate exhibited a regular array of square silicon micro-convexes (bright squares), and then the L-modified substrate showed a thin film on the surface. Comparing SEM images of

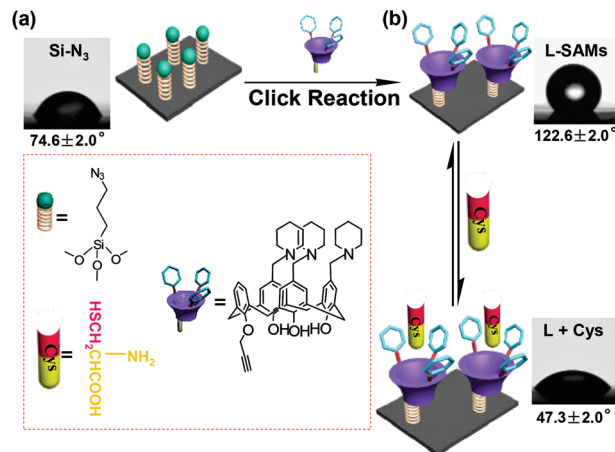


**Fig. 7** (a) Clicking L onto the silicon surface, which indicated that piperidine-calix[4]arene (L) was successfully modified on the silicon surface by the click reaction. (b) Constructing the [L + Cys] complex, which indicated a significant change in the CA between hydrophobicity and hydrophilicity.

the rough silicon surface before and after modification with L, the results indicated that L was successfully modified on the silicon surface. Moreover, the water-drop profiles showed different CAs on bare silicon wafer and the L-SAMs surface (Fig. S12†). This also proved the above conclusion.

In view of the extraordinary structure of L, we designed a Cys complex of piperidine-calix[4]arene on the functional silicon surface, and then the above metal ions were selected as guests because of the strong interaction between some metal ions and Cys. This process from hydrophilicity to hydrophobicity was proved by CA. Cys aqueous solution was added dropwise onto the modified silicon surface; 15 min later, the CA was  $47.3 \pm 2.0^\circ$ , then the [L + Cys] complex was constructed (Fig. 7b). The complex acted as a recognition ensemble toward  $\text{Hg}^{2+}$  against  $\text{Pb}^{2+}$ ,  $\text{Cd}^{2+}$ ,  $\text{Cu}^{2+}$ ,  $\text{Ni}^{2+}$ ,  $\text{Zn}^{2+}$  and  $\text{Ba}^{2+}$ . The complex showed a wettability response and selectivity for  $\text{Hg}^{2+}$  by CA measurements (Fig. 8a). At the same time, the corresponding CA variation [ $\Delta\text{CA} = (\text{CA}_0 - \text{CA})/\text{CA}_0$ ] ( $\text{CA}_0$  stood for contact angle of the [L + Cys] complex) histogram for the [L + Cys] complex with 7 different metal ions revealed a highly selective switch for  $\text{Hg}^{2+}$  (Fig. 8b). In addition, the L-SAMs surface which was immersed in Cys aqueous solution and sequentially reverted to  $\text{Hg}^{2+}$  aqueous solution could switch reversibly between hydrophobicity ( $122.6 \pm 2.0^\circ$ ) and hydrophilicity ( $47.3 \pm 2.0^\circ$ ). According to these results, a cycling experiment (Fig. S14†) between Cys and  $\text{Hg}^{2+}$  on the L-modified silicon surface was carried out, which switched cycles 6 times (Fig. 8c) and indicated a good reversible change between hydrophobicity and hydrophilicity. These results also indicated that Cys was successfully removed by  $\text{Hg}^{2+}$  from the [L + Cys] complex. Furthermore, the CAs of the [L + Cys] complex with various concentrations of  $\text{Hg}^{2+}$  (between  $1.0 \times 10^{-2}$  and  $1.0 \times 10^{-6}$  mol L<sup>-1</sup>) from hydrophobicity to hydrophilicity clearly showed that the detection limit for  $\text{Hg}^{2+}$  was  $1.0 \times 10^{-6}$  mol L<sup>-1</sup> (Fig. S15†).

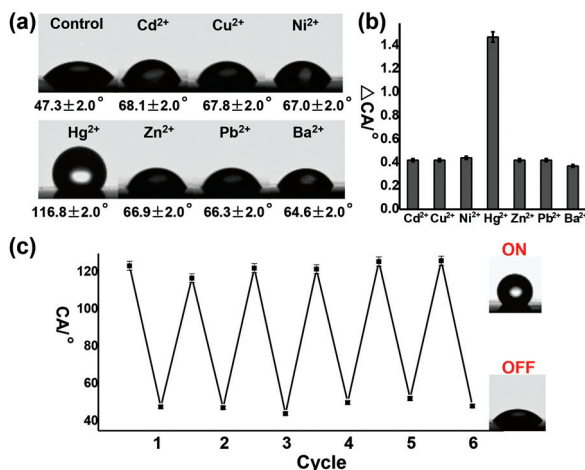


**Fig. 8** (a) CAs for the [L + Cys] complex (control) with 7 different metal ions. The error range of CAs was  $\pm 2.0^\circ$ . Note: the following error range of CAs was the same. (b) CA variation  $[\Delta CA = (CA_0 - CA)/CA_0]$  ( $CA_0$  stood for contact angle of the [L + Cys] complex) histogram for the [L + Cys] complex with 7 different metal ions, which showed a highly selective switch for Hg<sup>2+</sup> based on the Cys complex. (c) A cycling experiment of the wettability switch between Cys and Hg<sup>2+</sup> on the L-modified silicon surface, which exhibited a selective switch for Hg<sup>2+</sup> through multiple reversible cycles on the functional silicon surface.

To substantiate the role of the piperidine moiety within L in the recognition process, the control experiments were undertaken. The reference compound C4AM was adopted in the same method with Cys. CA and <sup>1</sup>H NMR measurements for C4AM in the presence of Cys were studied. As can be seen from Fig. S17 and S8,† they showed only small change upon addition of Cys. Thus, the results of the control experiments indicated that the piperidine moiety played an important role in the efficient interaction with Cys. To obtain further insight into the interaction, some other control experiments were performed. Moreover, some control experiments of CA were carried out with other biologically relevant molecules containing -SH, viz., cysteamine (CS), mercaptoacetic acid (MPA) and N-acetyl-L-cysteine (NAC) (Fig. 9 and Fig. S16†). These results

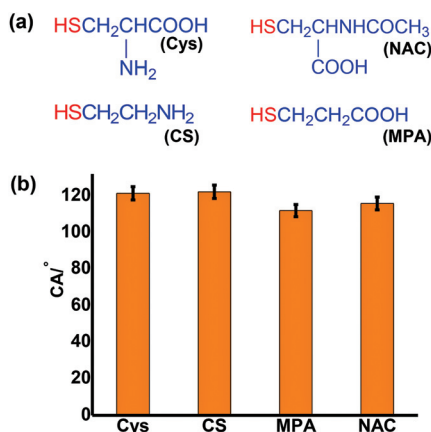


**Fig. 9** (a) The structure of different thiols. (b) The histogram showed CA changes of Hg<sup>2+</sup> with different thiols. These results suggested that the [L + Cys] complex was selective for only Hg<sup>2+</sup> owing to its unique Hg<sup>2+</sup>...SH interaction.

suggested that the [L + Cys] complex was selective only for Hg<sup>2+</sup> owing to its unique Hg<sup>2+</sup>...SH interaction. The highly selective wettability switch of the [L + Cys] complex toward Hg<sup>2+</sup> had been demonstrated by the above methods. The addition of Cys to L showed significant a switch off CA, and the CA was regained when Hg<sup>2+</sup> was added to result in the switch on mode. The result clearly demonstrated the reversible property of the [L + Cys] complex toward Hg<sup>2+</sup>.

## Conclusions

In summary, a novel piperidine-calix[4]arene complex (L) had been successfully synthesized for the first time. It exhibited strong binding toward Cys. Subsequently, the [L + Cys] complex was constructed. This had been demonstrated by FL, <sup>1</sup>H NMR spectroscopy and DFT computational studies. The [L + Cys] complex was selective toward Hg<sup>2+</sup>, over six other important heavy metal ions, viz., Pb<sup>2+</sup>, Cd<sup>2+</sup>, Cu<sup>2+</sup>, Ni<sup>2+</sup>, Zn<sup>2+</sup> and Ba<sup>2+</sup>. This was verified by FL, CA, <sup>1</sup>H NMR spectroscopy and AFM experiments. Thus, the present study demonstrated the utility of the [L + Cys] complex as a highly selective switch for Hg<sup>2+</sup> by exhibiting dual-signal reversible cycles. Most importantly, the [L + Cys] complex could act as a convenient and effective wettability switch for Hg<sup>2+</sup> on the functional micro-nano silicon surface. The recognition process and method can be used in many fields, such as biomimetics, environmental monitoring, clinical medicine and so on.<sup>18</sup>

## Experimental section

### 1. Materials and instruments

<sup>1</sup>H NMR and <sup>13</sup>C NMR spectra were recorded using a Varian Mercury VX400 instrument at ambient temperature with TMS as the internal standard. ESI-MS was carried out using a Finnigan LCQ-Advantage instrument. The static water contact angles were measured at 25 °C by means of an OCA 20 contact angle system (Dataphysics, Germany). FL spectra were recorded using a Type Cary Eclipse instrument. XPS was recorded on a KRATOS XSAM800 Electron spectrometer (FRR mode).

All chemicals were of A.R. grade and were purified by standard procedures. Milli-Q water was used to prepare all solutions in this study.

### 2. The synthesis of organic compounds

**The procedure for the synthesis of calix[4]arene (C4AM).** Calix[4]arene (C4DT) (2.4 mmol) was completely dissolved in acetonitrile and then sodium methylate (2.8 mmol) was added before stirring and refluxing for 0.5 h. Subsequently, propargyl bromide (0.5 mL) was added, then the mixture was stirred for 8 h. The crude product was purified by column chromatography (SiO<sub>2</sub>, petroleum ether-chloroform = 3/1) to afford propargyl-calix[4]arene (C4AM) in 85% yield. <sup>1</sup>H NMR (400 MHz, CDCl<sub>3</sub>):  $\delta$  9.67 (s, 1H, ArOH), 9.08 (s, 2H, ArOH), 7.09–6.98 (m, 9H, ArH), 6.69 (s, 3H, ArH), 4.95 (s, 2H, ArOCH<sub>2</sub>), 4.49–4.46 (d,

$J = 13.2$  Hz, 2H, ArCH<sub>2</sub>Ar), 4.29–4.25 (d,  $J = 18.9$  Hz, 2H, ArCH<sub>2</sub>Ar), 3.49–3.46 (d,  $J = 13.8$  Hz, 4H, ArCH<sub>2</sub>Ar), 2.75 (s, 1H, C≡CH). Anal. Calc. for C<sub>31</sub>H<sub>26</sub>O<sub>4</sub>: C, 80.50; H, 5.67. Found: C, 80.42; H, 5.52%.

**The procedure for the synthesis of piperidine-calix[4]arene (L).** C4AM (1.0 mmol) was completely dissolved in THF and then acetic acid (5.0 mmol) was added. Subsequently, piperidine (5.0 mmol) was added dropwise into the system. Later, formaldehyde (5.0 mmol) was added and the mixture was stirred for 8 h. Finally, complex **L** was produced. The product was purified by column chromatography (SiO<sub>2</sub>, ethyl acetate-petroleum ether = 2/10) giving a white powder **L** with a yield of 86%. <sup>1</sup>H NMR (600 MHz, DMSO):  $\delta$  6.99 (s, 2H, ArH), 6.87–6.79 (d,  $J = 16.0$  Hz, 4H, ArH), 6.71–6.69 (d,  $J = 7.3$  Hz, 2H, ArH), 6.48 (s, 1H, ArH), 4.55 (s, 2H, ArOCH<sub>2</sub>), 4.47 (d,  $J = 11.8$  Hz, 2H, ArCH<sub>2</sub>Ar), 4.05 (d,  $J = 12.3$  Hz, 2H, ArCH<sub>2</sub>Ar), 3.44 (s, 6H, ArCH<sub>2</sub>N), 3.13–3.08 (m, 4H, ArCH<sub>2</sub>Ar), 2.61 (s, 1H, C≡CH), 1.53 (m, 20H, (CH<sub>2</sub>)<sub>2</sub>N), 1.40–1.01 (m, 10H, (CH<sub>2</sub>)<sub>2</sub>N). <sup>13</sup>C NMR (150 MHz, DMSO):  $\delta$  156.70, 156.34, 155.59, 135.89, 132.59, 132.42, 132.15, 132.07, 131.59, 130.76, 129.51, 124.44, 80.56, 76.90, 64.04, 63.32, 54.51, 54.34, 49.48, 49.34, 49.13, 49.05, 48.91, 35.05, 32.97, 25.55, 25.51, 25.35, 24.53, 24.15. EI (+) MS  $m/z = 753.4$  ([M] + 80%) Anal. Calc. for C<sub>49</sub>H<sub>59</sub>N<sub>3</sub>O<sub>4</sub>: C, 78.05; H, 7.89; N, 5.57. Found: C, 77.94; H, 7.79; N, 5.43%.

### 3. Fluorescence experiments

All experiments of fluorescence cycles were carried out at an excitation wavelength of 350 nm using a fluorescence spectrometer and a 1 cm quartz cell. A bulk solution ( $1.0 \times 10^{-3}$  M, 2 mL) of Cys-F was freshly made before each set of experiments. **L** solution ( $1.0 \times 10^{-2}$  M) was made by dissolving **L** in CH<sub>3</sub>CN (1.2 mL). The Hg<sup>2+</sup> solutions were made at  $1.0 \times 10^{-2}$  M in water (1.2 mL). The fluorescence titrations were carried out by exciting the solution at 350 nm after adding the appropriate volume (20  $\mu$ L) of **L** solution to measure the fluorescence. Then the Hg<sup>2+</sup> solution (20  $\mu$ L) was added to the above mixed solution to measure the fluorescence, which showed fluorescence recovery over 6 switching cycles.

### 4. DFT computational details

The calculations reported in this article were performed at the B3LYP/6-31G(d) level using the Gaussian03 program package. The compound **L** (cone) was employed for geometry optimizations, then the complex formed between **L** and Cys was also optimized with the B3LYP/6-31G(d) method.

### 5. Preparation of the Si–N<sub>3</sub>-modified silicon substrates

**Fabrication of the micro–nano Si interface.** A silicon wafer was used directly as the smooth substrate. The structured silicon substrate was fabricated by the combination of photolithography and inductively coupled plasma (ICP) deep etching techniques. The photolithography and ICP techniques were used to obtain the patterned silicon micropillar structure on the silicon wafer. A rough surface introduced geometrical structures with patterned square pillars on a flat silicon wafer,

20  $\mu$ m high, 9  $\mu$ m long and with a spacing of 12  $\mu$ m between the silicon pillars.<sup>19</sup>

**Preparation of the Si–N<sub>3</sub>-modified silicon substrates.** Silicon substrates cut into 1 cm  $\times$  1 cm square pieces were soaked in chromosulfuric acid solution for 30–60 min and then rinsed with double distilled water and dried under a stream of N<sub>2</sub> gas. The cleaned wafers were immersed in aqueous NaOH (0.1 mol L<sup>-1</sup>) for 6 min and subsequently in HNO<sub>3</sub> (0.1 mol L<sup>-1</sup>) for 12 min to generate surface hydroxyl groups. After the silicon substrates had been washed with an excess of double distilled water and dried under a stream of N<sub>2</sub> flow, they were immersed in a refluxing solution of 5 wt% Si–N<sub>3</sub> in dry toluene (10 mL) at 110 °C for 6 h. Then they were washed with toluene and ethanol to remove the excess Si–N<sub>3</sub> and dried under a stream of N<sub>2</sub> gas.

**The click reaction between Si–N<sub>3</sub> and L on the silicon substrates.** The Si–N<sub>3</sub>-modified silicon surfaces were immersed in **L** solution in ethanol at 10<sup>-2</sup> M, then the mixture of copper sulfate (10<sup>-6</sup> M) and sodium ascorbate (10<sup>-7</sup> M) were added into this solution, which was then heated at 75 °C for 8 h. Then the silicon wafer was washed with a little ethanol and dried under a stream of N<sub>2</sub> gas.

### Conflict of interest

The authors declare no competing financial interest.

### Acknowledgements

This work was financially supported by the National Natural Science Foundation of China (21072072, 21102051), PCSIRT (no. IRT0953), Program for New Century Excellent Talent in University (NCET-10-0428).

### Notes and references

- (a) J. Gutknecht, *J. Membr. Biol.*, 1981, **61**, 61; (b) P. B. Tchounwou, W. K. Ayensu, N. Ninashvili and D. Sutton, *Environ. Toxicol. Chem.*, 2003, **18**, 149.
- W. B. Lu, X. Y. Qin, S. Liu, G. H. Chang, Y. W. Zhang, Y. L. Luo, A. M. Asiri, A. O. Youbi and X. P. Sun, *Anal. Chem.*, 2012, **84**, 5351.
- A. K. Mandal, M. Suresh, P. Das, E. Suresh, M. Baidya, S. K. Ghosh and A. Das, *Org. Lett.*, 2012, **14**, 2980.
- J. S. Wu, I. Hwang, K. S. Kim and J. S. Kim, *Org. Lett.*, 2007, **9**, 907.
- (a) L. Feng, S. H. Li, H. J. Li, J. Zhai, Y. L. Song, L. Jiang and D. B. Zhu, *Angew. Chem., Int. Ed.*, 2002, **41**, 1221; (b) F. Xia and L. Jiang, *Adv. Mater.*, 2008, **20**, 2842; (c) Y. Guo, F. Xia, L. Xu, J. Li, W. S. Yang and L. Jiang, *Langmuir*, 2010, **26**, 1024; (d) G. Y. Qing, X. Wang, H. Fuchs and T. L. Sun, *J. Am. Chem. Soc.*, 2009, **131**, 8370; (e) X. Hong, X. F. Gao and L. Jiang, *J. Am. Chem. Soc.*, 2007, **129**, 1478.

- 6 (a) T. L. Sun, G. J. Wang, L. Feng, B. Q. Liu, Y. M. Ma, L. Jiang and D. B. Zhu, *Angew. Chem., Int. Ed.*, 2004, **43**, 357; (b) D. G. Kurth and T. Bein, *Langmuir*, 1993, **9**, 2965.
- 7 M. Saadioui and V. Bohmer, *Calixarenes 2001*, 2001, 130.
- 8 F. Billes and I. M. Ziegler, *Supramol. Chem.*, 2002, **14**, 451.
- 9 N. M. Feng, H. Y. Zhao, J. Y. Zhan, D. M. Tian and H. B. Li, *Org. Lett.*, 2012, **14**, 1958.
- 10 R. K. Pathak, V. K. Hinge, K. Mahesh, A. Rai, D. Panda and C. P. Rao, *Anal. Chem.*, 2012, **84**, 6907.
- 11 (a) G. F. Zhang, J. Y. Zhan and H. B. Li, *Org. Lett.*, 2011, **13**, 3392; (b) F. J. Miao, J. Zhou, D. M. Tian and H. B. Li, *Org. Lett.*, 2012, **14**, 3572; (c) G. F. Zhang, X. L. Zhu, F. J. Miao, D. M. Tian and H. B. Li, *Org. Biomol. Chem.*, 2012, **10**, 3185.
- 12 (a) J. F. Callan, A. P. Silva and D. C. Magri, *Tetrahedron*, 2005, **61**, 8551; (b) A. Senthilvelan, M. T. Tsai, K. C. Chang and W. S. Chung, *Tetrahedron Lett.*, 2006, **47**, 9077.
- 13 S. Kanamathareddy and C. D. Gutsche, *J. Org. Chem.*, 1996, **61**, 2511.
- 14 A. M. Zeynep, *Anal. Sci.*, 2011, **27**, 277.
- 15 F. J. Miao, J. Y. Zhan, Z. L. Zou, D. M. Tian and H. B. Li, *Tetrahedron*, 2012, **68**, 2409.
- 16 M. J. Frisch, G. W. Trucks, H. B. Schlegel, G. E. Scuseria, M. A. Robb, J. R. Cheeseman, J. A. Montgomery Jr., T. Vreven, K. N. Kudin, J. C. Burant, J. M. Millam, S. S. Iyengar, J. Tomasi, V. Barone, B. Mennucci, M. Cossi, G. Scalmani, N. Rega, G. A. Petersson, H. Nakatsuji, M. Hada, M. Ehara, K. Toyota, R. Fukuda, J. Hasegawa, M. Ishida, T. Nakajima, Y. Honda, O. Kitao, H. Nakai, M. Klene, X. Li, J. E. Knox, H. P. Hratchian, J. B. Cross, V. Bakken, C. Adamo, J. Jaramillo, R. Gomperts, R. E. Stratmann, O. Yazyev, A. J. Austin, R. Cammi, C. Pomelli, J. Ochterski, P. Y. Ayala, K. Morokuma, G. A. Voth, P. Salvador, J. J. Dannenberg, V. G. Zakrzewski, S. Dapprich, A. D. Daniels, M. C. Strain, O. Farkas, D. K. Malick, A. D. Rabuck, K. Raghavachari, J. B. Foresman, J. V. Ortiz, Q. Cui, A. G. Baboul, S. Clifford, J. Cioslowski, B. B. Stefanov, G. Liu, A. Liashenko, P. Piskorz, I. Komaromi, R. L. Martin, D. J. Fox, T. Keith, M. A. Al-Laham, C. Y. Peng, A. Nanayakkara, M. Challacombe, P. M. W. Gill, B. G. Johnson, W. Chen, M. W. Wong, C. Gonzalez and J. A. Pople, *GAUSS-SIAN 03 (Revision C.02)*, Gaussian, Inc., Wallingford, CT, 2004.
- 17 M. Watson, J. Lyskawa, C. Zobrist, D. Fournier, M. Jimenez, M. Traisnel, L. Gengembre and P. Woisel, *Langmuir*, 2010, **26**, 15920.
- 18 (a) D. C. Apodaca, R. B. Pernites, F. R. Mundo and R. C. Advincula, *Langmuir*, 2011, **27**, 6768; (b) Y. C. Tyan, M. H. Yang, T. W. Chung, W. C. Chen, M. C. Wang, Y. L. Chen, S. L. Huang, Y. F. Huang and S. B. Jong, *J. Mater. Sci.: Mater. Med.*, 2011, **22**, 1383; (c) X. P. He, X. W. Wang, X. P. Jin, H. Zhou, X. X. Shi, G. R. Chen and Y. T. Long, *J. Am. Chem. Soc.*, 2011, **133**, 3649; (d) L. Basabe-Desmonts, F. V. D. Baan, R. S. Zimmerman, D. N. Reinhoudt and M. Crego-Calama, *Sensors*, 2007, **7**, 1731.
- 19 G. Y. Qing, X. Wang, H. Fuchs and T. L. Sun, *J. Am. Chem. Soc.*, 2009, **131**, 8370.